Fluid Phase Equilibria 299 (2010) 285–293

Contents lists available at ScienceDirect

Fluid Phase Equilibria

journal homepage: www.elsevier.com/locate/fluid

SRK equation of state: Predicting binary interaction parameters of hydrocarbons and related compounds

Giorgio Soave[a,*], Simone Gamba[b], Laura A. Pellegrini[b]

[a] Via Europa 7, I-20097 San Donato Milanese, Italy
[b] Dipartimento di Chimica, Materiali e Ingegneria Chimica "G. Natta", Politecnico di Milano, Piazza Leonardo da Vinci 32, I-20133 Milano, Italy

ARTICLE INFO

Article history:
Received 25 May 2009
Received in revised form 6 September 2010
Accepted 7 September 2010
Available online 17 September 2010

Keywords:
Equation of state
Cubic
Mixing rules
Group contributions

ABSTRACT

The parameter mixing rules of the Soave–Redlich–Kwong (SRK) equation of state are rewritten as Huron–Vidal mixing rules, where infinite-pressure activity coefficients are predicted by group contributions. Alkanes are treated as composed by one group type and aromatics by two types, aliphatic and aromatic. Hydrocarbon mixtures can be treated using one universal interaction parameter. Light compounds like methane, N_2, CO_2, H_2S, etc. are treated as separate groups; each one requires a pair of parameters for its interactions with aliphatic and aromatic groups. Group interaction parameters were determined from experimental VLE data. From them, binary interaction constants of the classical quadratic mixing rules can directly be derived.

1. Introduction

A widely applied equation of state (EoS) is the Soave–Redlich–Kwong (SRK) one [1]:

$$P = \frac{RT}{v-b} - \frac{a}{v(v+b)} \tag{1}$$

The so-called 'classical' parameter mixing rules:

$$a = \sum_i \sum_j x_i x_j a_{ij} = \sum_i \sum_j x_i x_j (1-k_{ij}) \sqrt{a_i a_j} \tag{2}$$

$$b = \sum_i x_i b_i \tag{3}$$

can give a satisfactory description of the vapor–liquid-equilibrium (VLE) behaviour of systems formed by hydrocarbons and related compounds like nitrogen, carbon dioxide and hydrogen sulfide. For its simplicity it is widely applied for process design in the hydrocarbon field.

Binary parameters k_{ij} are not known in general, however. Relatively few values have been determined by correlation of experimental VLE data and are reported in the literature (e.g., [2]). Zero values of k_{ij} can be, and usually are, applied for alkane–alkane pairs, but for others (especially those including non-hydrocarbons) they should be different from zero and they have to be determined; that requires to retrieve and correlate experimental VLE data of each pair of compounds, a practically impossible task.

For that reason methods have been developed in the last decades, which determine the parameters of the Redlich–Kwong or the Peng–Robinson EoSs from activity coefficients predicted by the UNIFAC model which had to be extended to light compounds (hydrogen, nitrogen, carbon oxides, etc.). Two methods were made available by Gmehling and co-workers: the widely applied PSRK method [3] and the more recent and still incomplete VTPR method [4] based on the Peng–Robinson EoS. In principle, they enable to predict the phase equilibrium and other thermodynamic properties of a wide variety of systems.

This work was mainly aimed to develop a tool to predict EoS parameters from a small number of universal group interaction parameters. The new method is restricted to hydrocarbons and related components (N_2, CO_2, H_2S), i.e., systems where the classical quadratic mixing rules apply. It can be used to directly estimate parameters of the SRK EoS, or the binary interaction parameters k_{ij} for the classical mixing rules.

2. The Huron–Vidal mixing rules

Many years ago Huron and Vidal [5] proposed a different type of mixing rules for the SRK EoS. They assumed that the excess properties of mixtures have a finite limit at infinite pressure. The rules they derived from that, gave rise to the mixing rules expressed by

* Corresponding author. Tel.: +39 02 55602870.
E-mail address: Giorgio_Soave@virgilio.it (G. Soave).

0378-3812/$ – see front matter © 2010 Elsevier B.V. All rights reserved.
doi:10.1016/j.fluid.2010.09.012

Eq. (3) and:

$$\frac{a}{b} = \sum_i x_i \left(\frac{a_i}{b_i}\right) - \Lambda g^{E\infty} = \sum_i x_i \left(\frac{a_i}{b_i} - \Lambda RT \ln \gamma_i^{\infty}\right) \quad (4)$$

Λ depends on the type of two-parameter cubic EoS; for the SRK EoS, $\Lambda = 1/\ln 2 = 1.442695$.

$G^{E\infty}$ and γ^{∞} are hypothetical quantities expressing the deviations from the ideal-mixture behaviour at infinite pressure. They can be expressed by any of the models currently applied to describe liquid mixtures. If the model for $g^{E\infty}$ is flexible enough, strongly non-ideal systems can accurately be described. But, whichever is the $g^{E\infty}$ model, its interaction parameters are not known, so the problem of predicting mixtures' behaviour is left unresolved.

This paper started from the consideration that the classical mixing rules are a particular case of the H–V mixing rules. In fact, applying them in Eq. (4) we have:

$$\Lambda g^{E\infty} = \sum_i x_i \frac{a_i}{b_i} - \frac{a}{b} = \sum_i x_i \frac{a_i}{b_i} - \frac{\sum_i \sum_j x_i x_j a_{ij}}{\sum_i x_i b_i}$$

$$= \frac{\sum_i \sum_j x_i x_j b_i b_j \left(\frac{1}{2}\frac{a_i}{b_i^2} + \frac{1}{2}\frac{a_j}{b_j^2} - \frac{a_{ij}}{b_i b_j}\right)}{\sum_i x_i b_i} \quad (5)$$

or, briefly:

$$\frac{g^{E\infty}}{RT} = \frac{\sum_i \sum_j x_i x_j b_i b_j \tau_{ij}/2}{\sum_i x_i b_i} = \left(\sum_i x_i b_i\right)\left(\sum_i \sum_j \frac{\phi_i \phi_j \tau_{ij}}{2}\right) \quad (6)$$

where

$$\phi_i = \frac{x_i b_i}{\sum x_j b_j} \quad (7)$$

From Eq. (5):

$$\ln \gamma_i^{\infty} = \left[\frac{\partial}{\partial n_i}\left(n_T \frac{g^{E\infty}}{RT}\right)\right]_{T,P,n_j}$$

$$= b_i \left(\sum_j \phi_j \tau_{ij} - \frac{1}{2}\sum_j \sum_k \phi_j \phi_k \tau_{jk}\right) \quad (8)$$

Eqs. (6)–(8) are identical to the Scatchard–Hildebrandt (S–H) equations [6] for regular solutions, with the only difference that liquid volumes v_i are replaced here by co-volumes b_i. In other words, the classical parameter mixing rules correspond to assuming a regular solution at infinite pressure.

Replacing the quadratic mixing rules by the equivalent Eqs. (6)–(8), the equation for fugacity coefficients in mixtures becomes:

$$\ln \varphi_i = \frac{b_i}{b}\left(\frac{Pv}{RT} - 1\right) - \log\left(\frac{P(v-b)}{RT}\right)$$

$$- \left(\frac{a_i}{RTb_i} - \Lambda \ln \gamma_i^{\infty}\right) \ln\left(1 + \frac{b}{v}\right) \quad (9)$$

Unlike k_{ij}, infinite-pressure activity coefficients can be predicted by the use of group contributions, as it is shown in Section 3. Thus the SRK EoS can be made predictive, while keeping the classical mixing rules.

3. Predicting γ^{∞} by the Theory of Group Solutions

The proposed method follows the rationale of the well-known UNIFAC method [7] by applying the Theory of Group Solutions [8]. According to it, the activity coefficient of each component of a mixture can be calculated by combining the activity coefficients (at infinite pressure, in our case) of its functional groups:

$$\ln \gamma_i = \sum \upsilon_{ki} (\ln \Gamma_k - \ln \Gamma_{ki}) \quad (10)$$

where υ_{ki} is the number of groups k in the component i; Γ_k is the activity coefficient of group k in the group mixture obtained from the mixture and Γ_{ki} is activity coefficient of group k in the group mixture obtained from the pure component i.

While UNIFAC considered low-pressure solutions and used the UNIQUAC equation [9] for Γ, the Scatchard–Hildebrandt [S–H] equation, Eq. (8), was applied here to express infinite-pressure activity coefficients. For the sake of simplicity, the same assumptions of UNIFAC were made, i.e., (1) groups forming hydrocarbons are collected into two group families or "main groups", namely alkyl groups CH_n and aromatic groups aCH_n; (2) groups belonging to the same main group do not interact each other; i.e., $\tau_{mn} = 0$ if m and n are referred to the same main groups; (3) groups belonging to the same main groups interact by the same strength with groups belonging to another main group; e.g., one τ_{mn} parameter is used to describe all alkyl–CO_2 or alkyl–aromatic interactions; (4) in addition, τ_{mn} parameters are symmetrical ($\tau_{mn} = \tau_{nm}$), which means one parameter for each pair of main groups. That drastically reduces the number of interaction parameters to be determined: (1) one τ_{mn} for all aromatic–aliphatic pairs; (2) two τ_{mn} parameters for the interactions of aliphatic and aromatic groups with either methane or N_2, CO_2, H_2S.

With the above assumptions, each system is reduced to a solution of groups formed by alkyl groups, aromatic groups and one group each for methane, N_2, CO_2, H_2S.

Note that no assumption is needed for b values of the groups N_2, CO_2, H_2S and methane; they are directly calculated from critical constants. Also an alkane can be treated as a single group, whose dimensions are equal to its covolume. Only the covolumes of aromatic compounds have to be shared between an aliphatic and an aromatic part; that will be discussed further on.

As it can be seen from Eqs. (6) and (8), interaction parameters τ_{mn} are inversely proportional to the numerical values assumed for the covolumes b which depend on the units of T_c and P_c. So, in order to simplify calculations, the covolumes $b = .08664\, RT_c/P_c$ (cm^3/mol) were replaced by the reduced covolumes $b' = (T_c/P_c)$ (K/bar) which are proportional to them. The interaction parameters τ were scaled in accordance and were expressed as (bar/K).

Finally, the law of dependence on the temperature of the interaction parameters τ had to be defined. Instead of the more common law like $\tau_{mn} = a_{mn} + b_{mn}/T$ which was found to give too weak a dependence on the temperature, a more flexible equation was adopted:

$$\tau_{mn}\left(\frac{\text{bar}}{\text{K}}\right) = \left(\frac{a_{mn}}{T(\text{K})}\right)^{b_{mn}} \quad (11)$$

where the exponent b_{mn} varies usually between 1 and 2, depending on the group pair.

4. Determination of the interaction parameters

Experimental VLE data from the literature were tested and less reliable data rejected. For each data set the attractive parameters a_i of components (see Eq. (9)) were adjusted to reproduce their experimental vapour pressures [10]; when they were missing from the data set, reliable values were taken from the literature and added to the data set. If the temperature was higher than the critical temperature of one component, its attractive parameter was calculated using the classical SRK equation [1]. With such assumptions the

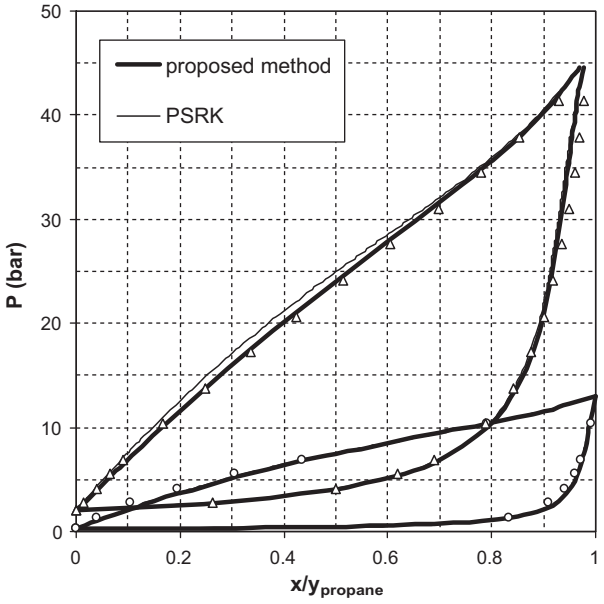

Fig. 1. Propane–benzene at 310.93 and 377.59 K. Symbols: experimental [12], lines: predicted by Eq. (12) and PSRK.

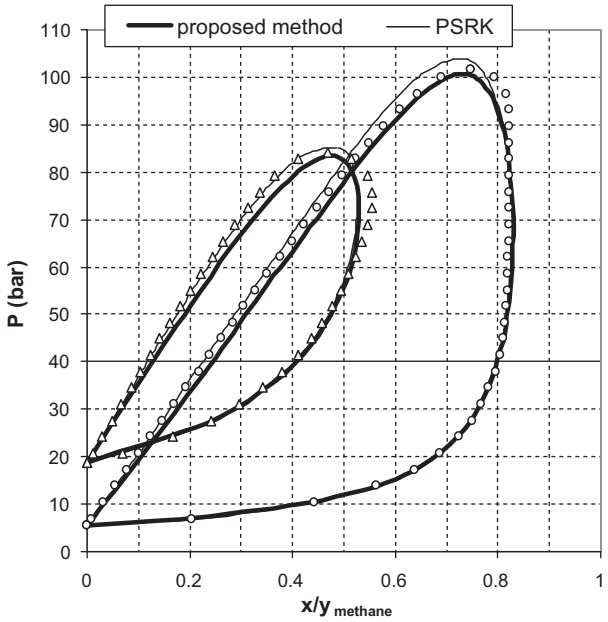

Fig. 2. Methane–propane at 277.59 and 327.59 K. Symbols: experimental [13], lines: predicted by Eq. (13) and PSRK.

data were correlated to determine the best a_{mn}, b_{mn} parameters of Eqs. (6)–(11).

Owing to the need of processing data related to systems with different components and relative volatilities, the correlations were not carried out by minimizing the root mean square (RMS) ΔP of bubble-pressure calculations, but according to a simplified Maximum Likelihood method, minimizing the root mean square weighted (RMSW) ΔP, where single bubble-point ΔP were replaced by the approximated orthogonal distances of the experimental points to the calculated P–x curve. That means to give a higher weight to the ΔP of systems with lower relative volatilities, which are more important from a fractionation point of view. The procedure is described in Appendix A. By an exam of the calculated phase envelopes it was concluded that values below 0.01 of the RMSW ΔP can be considered satisfactory, regardless of the RMS ΔP.

Paragraphs 4.1–4.15 report the results of calculations carried out by applying Eqs. (6)–(11).

Some results are graphically shown in Figs. 1–10, together with predictions by the well-known PSRK method [3]. Results for the PSRK method have been obtained by using the Aspen Properties® software (V7.1) [11]. Comparisons show equivalent accuracy.

The procedure for the determination of k_{ij} from Eqs. (6)–(11) is discussed in Section 5.

4.1. Alkanes/aromatic hydrocarbons

Aliphatic and aromatic groups are present in most hydrocarbon systems and their interactions are relatively weak, so the related interaction parameter was determined first. A preliminary value was determined from VLE data of benzene with n-alkanes C_5–C_7 (benzene contains only aromatic groups and no assumption is needed on how to split its reduced covolume b'). Selected experimental data (496 data points) were correlated accurately by:

$$\tau\left(\frac{\text{aromatic}}{\text{alkane}}\right) = \left(\frac{72}{T}\right)^2 \tag{12}$$

where, from here on, τ is expressed in bar/K and the temperature is in degrees K. The average errors were: 0.21 K (isobars), 0.85% (isotherms) or, more significantly, RMSW ΔP = 0.0045.

Results remained accurate when Eq. (12) was tested on data of benzene with light alkanes, in spite of the relative inability of the classical quadratic mixing rules to describe unsymmetrical systems: RMSW ΔP = 0.0084 for ethane/benzene (104 pts.), 0.0075 for propane/benzene (81 pts.). See Fig. 1 for the propane/benzene system at 104 °C.

Results were satisfactory for systems with heavier alkanes up to dodecane as well.

Eq. (12) was then checked on systems involving higher aromatics, toluene first, requiring a statement of how to split their covolumes between the aliphatic and the aromatic part.

Let us consider toluene, the simplest case: $b' = T_c/P_c$ = 591.75/41.08 = 14.40 K/bar. The part attributed to the methyl was derived from ethane's b' = 305.32/48.72 = 6.267 K/bar. Hence $b'(CH_3)$ = 3.13. By difference, the contribution of the phenyl is 14.40–3.13 = 11.27 K/bar.

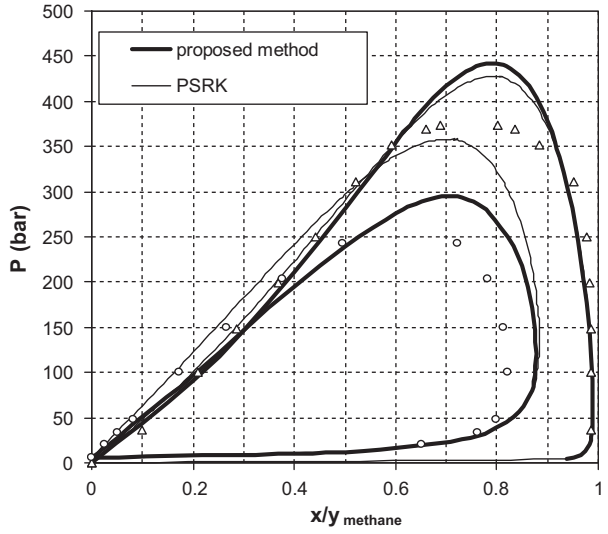

Fig. 3. Methane–benzene at 313.2 and 421.05 K. Symbols: experimental [14,15], lines: predicted by Eq. (14) and PSRK.

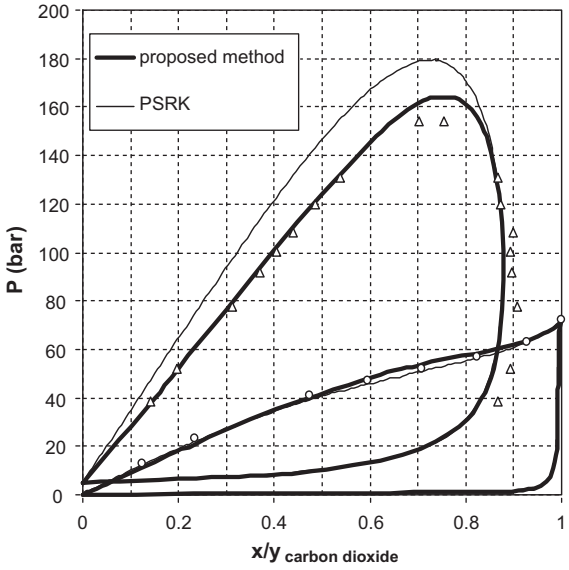

Fig. 4. CO_2–benzene at 303.15 and 413.6 K. Symbols: experimental [16,17], lines: predicted by Eq. (17) and PSRK.

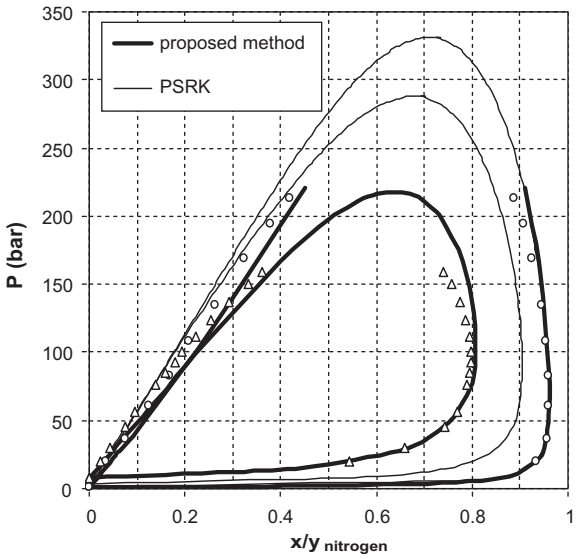

Fig. 6. N_2–propane at 230 and 260 K. Symbols: experimental [19], lines: predicted by Eq. (20) and PSRK.

Using that value the application of Eq. (12) to alkane/toluene data was satisfactory: RMSW $\Delta P = 0.0023$ for benzene/toluene data and lower than 0.01 for toluene/alkane data, including light alkanes. Equally good results were given for alkane/alkylbenzene systems.

A problem arose with polyalkylbenzenes, first the three xylenes. Although they have the same molecular structure, their b' values are different: 630.3/37.32 = 16.89 K/bar for o-xylene, 617.0/35.41 = 17.42 K/bar m-xylene, 616.2/35.11 = 17.55 K/bar p-xylene. Whichever is the choice for splitting their covolume, their aromatic fraction and hence their interactions with other compounds will be different. Calculations proved that, like with alkylbenzenes, best results are obtained by assuming a fixed part 11.27 K/bar for the aromatic part (so neglecting its different number of hydrogen atoms) and letting the difference from the total b' to the aliphatic part (which is a notable simplification). Results were satisfactory for alkane/xylene systems as well: RMSW $\Delta P = 0.0066$ for o-xylene/heptane, 0.0024 for p-xylene/heptane but also 0.0081 for m-xylene/propane. The conclusion is that a universal value 11.27 K/bar can be used for the aromatic part of b' of all alkyl- and polyalkylbenzenes.

Eq. (12) can also be applied to systems containing polynuclear aromatic hydrocarbons, with some loss of confidence owing to the uncertainty of their critical constants. Naphthalene can be treated as a purely aromatic compound with $b' = 720/36.5 = 19.73$ K/bar. Results of VLE calculations using Eq. (12) were just acceptable (e.g., RMSW $\Delta P = 0.0400$ for naphthalene/tetradecane). Problems occurred when dealing with alkylnaphthalenes, decalin or other double-ring aromatics; so that matter was left apart.

4.2. Methane/alkanes

Preliminary trials showed that methane–alkane systems cannot be treated properly by treating methane like other alkanes. It was necessary to treat it as a separate main group and to define its interaction parameter with other main groups. Selected experimental

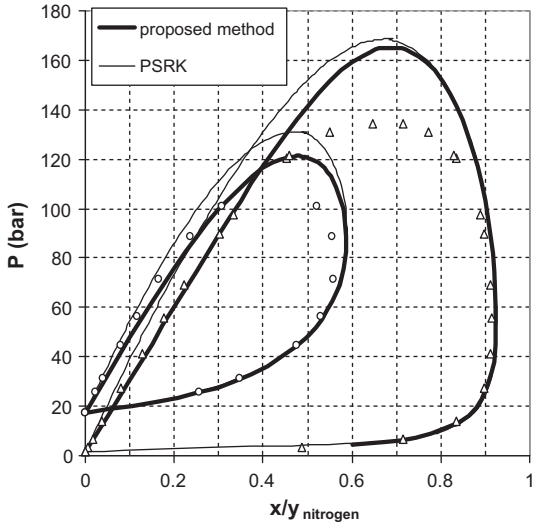

Fig. 5. N_2–ethane at 194.26 and 260 K. Symbols: experimental [18,19], lines: predicted by Eq. (20) and PSRK.

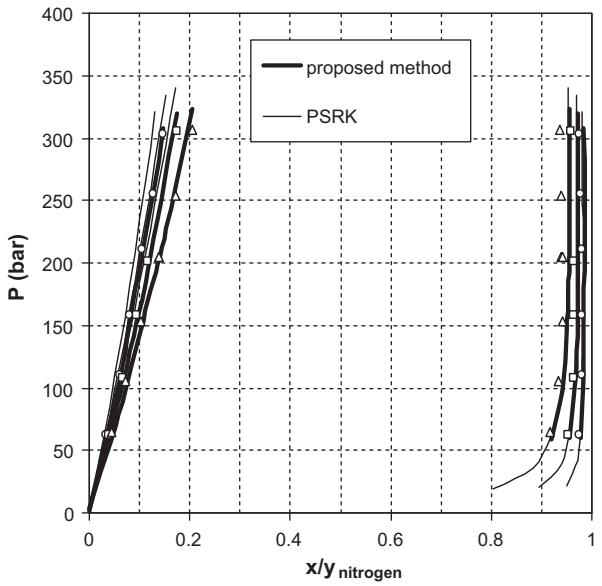

Fig. 7. N_2–benzene system at 348.15, 373.15, and 398.15 K. Symbols: experimental [20], lines: predicted by Eq. (21) and PSRK.

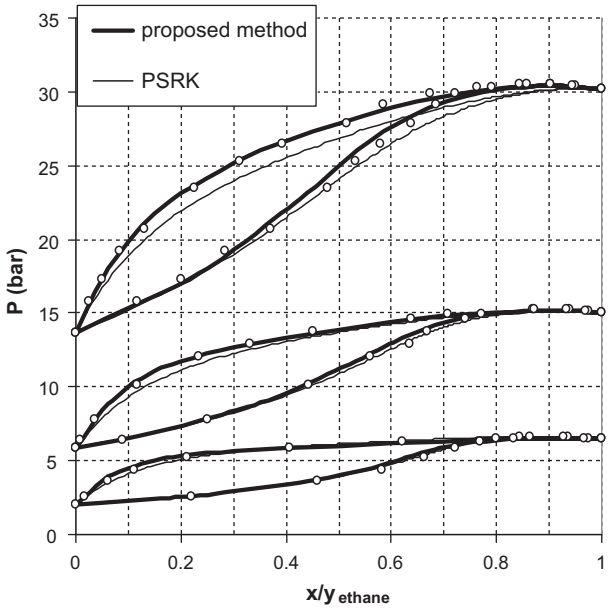

Fig. 8. Ethane–H_2S system at 227.93, 255.32, and 283.15 K. Symbols: experimental [21], lines: predicted by Eq. (25) and PSRK.

data of methane–ethane systems from 90.7 to 280 degrees K (193 points from 5 sources) were correlated well (RMSW $\Delta P = 0.0039$) by:

$$\tau\left(\frac{CH_4}{\text{alkanes}}\right) = \left(\frac{29}{T}\right)^2 \tag{13}$$

Eq. (13) was then applied to the methane–propane and methane–butane systems with satisfactory results, basing on the low values of the RMSW ΔP (0.0103 for methane–propane data, 207 pts., and 0.0080 for methane/n-butane, 300 pts.). E.g., see Fig. 2 for the methane–propane system.

Eq. (13) was thus assumed as the interaction parameter for all methane–alkane pairs.

In this particular case, also classical quadratic mixing rules with $k_{ij} = 0$ behaved properly.

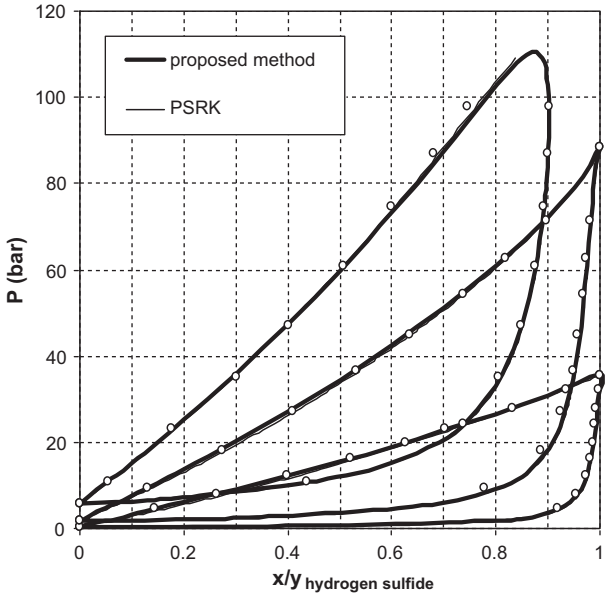

Fig. 9. H_2S–benzene system at 323.1, 372.6, and 422.6 K. Symbols: experimental [22], lines: predicted by Eq. (26) and PSRK.

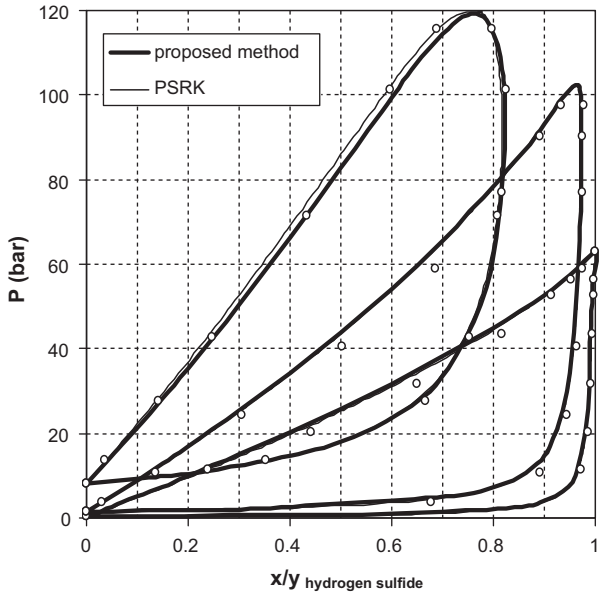

Fig. 10. H_2S–toluene at 352.59, 394.26, and 477.59 K. Symbols: experimental [23], lines: predicted by Eq. (26) and PSRK.

4.3. Methane/aromatic hydrocarbons

Correlations were made difficult by the scarcity of data and the inability of classical mixing rules to follow the whole phase envelope when relative volatilities are high, especially if one component is supercritical. In the former works that problem was overcome by treating first systems with close component volatilities but that was not possible for methane with aromatic compounds. The correlation of selected experimental methane–benzene data (46 pts from 3 sources) gave:

$$\tau\left(\frac{CH_4}{\text{aromatic}}\right) = \left(\frac{100}{T}\right)^2 \tag{14}$$

In spite of the very different volatilities the RMSW ΔP is 0.0093, acceptable. See Fig. 3.

Eq. (14) was then checked on methane–toluene and methane/m-xylene data with acceptable results (RMSW $\Delta P = 0.0133$ and 0.0118, respectively). So Eq. (14) can be assumed as the universal parameter for methane–aromatic interactions.

4.4. Methane/CO_2

Experimental data (60 pts. from 2 sources) were correlated accurately (RMSW $\Delta P = 0.0031$) by:

$$\tau\left(\frac{CH_4}{CO_2}\right) = \left(\frac{110}{T}\right)^{1.6} \tag{15}$$

4.5. CO_2/alkanes

The interaction parameter was determined from VLE data of the CO_2–ethane system (225 pts. from 5 sources), the most critical one. Data were tightly correlated (RMSW $\Delta P = 0.0045$) by:

$$\tau\left(\frac{CO_2}{\text{alkanes}}\right) = \left(\frac{118}{T}\right)^{1.6} \tag{16}$$

Eq. (16) was then successfully checked on systems with higher alkanes, up to decane, with RMSW ΔP values mostly below 0.01.

4.6. CO_2/aromatic hydrocarbons

The interaction parameter for the CO_2–aromatic pair was determined first from selected CO_2–benzene data (72 pts. from 3 sources). By data correlation (RMSW $\Delta P = 0.0102$):

$$\tau\left(\frac{CO_2}{\text{aromatic}}\right) = \left(\frac{116}{T}\right)^2 \quad (17)$$

An example is given in Fig. 4 for the CO_2–benzene system at 303.15 and 413.6 K.

Eq. (17) was then favourably checked on the available CO_2–toluene data (117 pts. from 3 sources) and CO_2–m-xylene data (39 points). RMSW $\Delta P = 0.0123$ and 0.0067 respectively. Eq. (17) was assumed as a universal parameter for the CO_2–aromatic interactions.

4.7. Nitrogen/CO_2

Owing to the relatively high triple point of CO_2, the temperature range of experimental data is restricted, from 218 to 293.15 K, all far over the critical temperature of nitrogen, what made the determination of the exponent of T uncertain in the equation for τ.

The correlation of selected experimental data (118 points from 6 sources) gave:

$$\tau\left(\frac{N_2}{CO_2}\right) = \left(\frac{85}{T}\right)^{1.2} \quad (18)$$

with a very low value of the RMSW ΔP (0.0024).

4.8. Nitrogen/methane

Experimental data are plentiful and accurate and cover a wide range of temperature. Selected data (260 pts. from 3 sources) were accurately correlated (RMSW $\Delta P = 0.0025$) by:

$$\tau\left(\frac{N_2}{CH_4}\right) = \left(\frac{18.0}{T}\right) \quad (19)$$

4.9. Nitrogen/alkanes

Experimental data are plentiful, but their correlation was hindered by the occurring of phase splitting at low temperatures and, again, the wide volatility differences which made it difficult to reproduce the full phase envelopes. Nitrogen/ethane data (210 data points from 110.9 to 290 K) were well correlated (RMSW $\Delta P = 0.0060$) by:

$$\tau\left(\frac{N_2}{\text{alkane}}\right) = \left(\frac{57}{T}\right)^{1.4} \quad (20)$$

See Fig. 5 for the nitrogen/ethane system at 194.26 and 260 K.

Then Eq. (20) was tested on higher alkanes (N_2/propane, 167 pts. from 4 sources, N_2/n-butane, 121 pts. from 4 sources, and N_2/hexane, 58 pts.) with less satisfactory results (RMSW $\Delta P = 0.0288$, 0.0170 and 0.0287 respectively). The calculated phase envelopes match acceptably the experimental ones, as shown in Fig. 6 for the N_2/butane at 310.9 K.

4.10. Nitrogen/aromatic hydrocarbons

The scarcity of experimental data and the wide differences of relative volatilities made it difficult to treat nitrogen/aromatic systems. Correlation of nitrogen/benzene data (21 points from one source) gave:

$$\tau\left(\frac{N_2}{\text{aromatic}}\right) = \left(\frac{163}{T}\right)^{1.6} \quad (21)$$

with RMSW $\Delta P = 0.0025$. See Fig. 7.

Less satisfactory, but still acceptable was its application to higher aromatics, owing to the above said reasons.

4.11. H_2S/N_2

Available experimental data (77 pts. from 2 sources) could be correlated accurately (RMSW $\Delta P = 0.0015$) by:

$$\tau\left(\frac{N_2}{H_2S}\right) = \left(\frac{198}{T}\right)^{1.3} \quad (22)$$

4.12. H_2S/CO_2

The correlation of data (190 pts. from 2 sources) was satisfactory (RMSW $\Delta P = 0.0053$):

$$\tau\left(\frac{CO_2}{S}\right) = \left(\frac{120}{T}\right)^{1.6} \quad (23)$$

4.13. H_2S/methane

Correlation of data (101 pts. from 2 sources) was satisfactory (RMSW $\Delta P = 0.0033$):

$$\tau\left(\frac{CH_4}{H_2S}\right) = \left(\frac{123}{T}\right)^{1.3} \quad (24)$$

4.14. H_2S/alkanes

Experimental data of the ethane–H_2S system (53 pts.) were accurately correlated (RMS $\Delta P = 2.81\%$, RMSW $\Delta P = 0.0062$; see also Fig. 8) by:

$$\tau\left(\frac{H_2S}{\text{alkane}}\right) = \left(\frac{114}{T}\right)^{1.4} \quad (25)$$

The accuracy of Eq. (25) is confirmed by an application to other H_2S/alkane data: RMSW $\Delta P = 0.0137$ for H_2S/propane, 0.0065 for H_2S/butane and around 0.01 for higher alkanes.

4.15. H_2S/aromatic hydrocarbons

Experimental data (101 pts.) of the H_2S–benzene system were accurately correlated (RMSW $\Delta P = 1.39\%$, RMSW $\Delta P = 0.0035$) with:

$$\tau\left(\frac{H_2S}{\text{aromatic}}\right) = \left(\frac{10}{T}\right) \quad (26)$$

Application of Eq. (26) to other H_2S–aromatic systems was satisfactory, with RMSW ΔP values a little over 0.01. See Fig. 9 (H_2S–benzene) and 10 (H_2S–toluene).

5. Estimating binary interaction parameter k_{ij} of the quadratic mixing rules

Finally, the predictive method developed here can be applied to determine binary interaction parameters k_{ij} of the classical quadratic mixing rules. That is done by comparing the fugacity coefficient equations determined from the classical mixing rules and the Huron–Vidal ones:

Classical:

$$\ln \varphi_i = \frac{b_i}{b_m}\left(\frac{Pv}{RT}-1\right) - \ln\left(\frac{P(v-b_m)}{RT}\right) - \left(2\frac{\sum_j x_j a_{ij}}{a_m} - \frac{b_i}{b_m}\right)\frac{a_m}{RTb_m}\ln\left(1+\frac{b_m}{v}\right) \quad (27)$$

Huron–Vidal:

$$\ln \varphi_i = \frac{b_i}{b_m}\left(\frac{Pv}{RT}-1\right) - \ln\left(\frac{P(v-b_m)}{RT}\right) - \left(\frac{a_i}{RTb_i} - \frac{\ln \gamma_i^{\infty}}{\ln 2}\right)\ln\left(1+\frac{b_m}{v}\right) \quad (28)$$

If the two mixing rules are equivalent, quantities a_m, b_m, and v are the same, so the equivalence condition reduces to:

$$\left(2\frac{\sum_j x_j a_{ij}}{a_m} - \frac{b_i}{b_m}\right)\frac{a_m}{RTb_m} = \left(\frac{a_i}{RTb_i} - \frac{\ln \gamma_i^{\infty}}{\ln 2}\right) \quad (29)$$

without any need of solving the cubic equation of state. The value of k_{12} given by Eq. (29) for a binary system is independent on the system composition; so it is simpler to consider the particular case of component 1 at infinite dilution in component 2, which avoids considering mixture parameters:

$$\left(2(1-k_{12})\sqrt{\frac{a_1}{a_2}} - \frac{b_1}{b_2}\right)\frac{a_2}{RTb_2} = \left(\frac{a_1}{RTb_1} - \frac{\ln \gamma_{1(2)}^{\infty}}{\ln 2}\right) \quad (30)$$

All terms in Eq. (30) are known but k_{12} at the left-hand member and $\gamma_{1(2)}^{\infty}$, which can be predicted by group contributions, at the right-hand member.

As an example Table 1 shows the values of k_{12} for the CO_2–propane pair at various temperatures using Eq. (16) to predict γ_1^{∞} of CO_2 at infinite dilution in propane. Below the component critical temperatures, the attractive parameters α could be more rigorously determined from experimental vapor pressures [10] but k_{12} values varied negligibly when the attractive parameters were calculated using the original SRK equations.

So from here on k_{12} will be calculated using the SRK equations for α.

An important remark is that k_{12} varies with temperature, so a temperature must be chosen for each component pair if a general-purpose value of k_{12} is wanted. In general it is advisable to use lower temperatures, where phase equilibria and thermodynamic properties are more sensitive to k_{12}. As a suggestion, the normal boiling point of the lighter component (or in the case of CO_2, its triple point), taking care not to go below the range of validity of equations for α, say, a reduced temperature 0.5 of the heavier component.

Table 1
k_{12} values for the CO_2–propane system.

T (K)	$P^{\circ}_{CO_2}$ (bar)	$P^{\circ}_{C_3H_8}$ (bar)	k_{12}
216.6	5.191	.5084	0.1329
220	6.005	.6038	0.1330
230	8.954	.9658	0.1336
240	12.86	1.478	0.1342
250	17.88	2.179	0.1349
260	24.22	3.108	0.1357
270	32.08	4.308	0.1366
280	41.69	5.823	0.1377
290	53.31	7.701	0.1390
300	67.25	9.989	0.1405

Table 2
k_{12} values for CO_2/alkane systems.

2nd component	T (K)	k_{12}
Ethane	216.6	0.1336
Propane	216.6	0.1329
n-Butane	216.6	0.1322
i-Butane	216.6	0.1284
n-Pentane	234.8	0.1316
i-Pentane	230.2	0.1300
n-Hexane	253.8	0.1315
n-Octane	284.3	0.1316
n-Decane	284.3	0.1316

Table 3
k_{12} values for CO_2/aromatic systems.

2nd component	T (K)	k_{12}
Benzene	281.0	0.0910
Toluene	295.9	0.0961
Ethylbenzene	308.6	0.1003
o-Xylene	315.1	0.0998
m-Xylene	308.5	0.1008
p-Xylene	308.1	0.1010
n-Propylbenzene	319.2	0.1042
i-Propylbenzene	315.5	0.1034
n-Butylbenzene	330.2	0.1079
Mesitylene	318.6	0.1049
Diphenyl	386.5	0.0873

Table 4
k_{12} values for methane/alkane systems (at a reduced temperature 0.5 of the heavier component).

2nd component	T (K)	k_{12}
Ethane	152.7	0.0026
Propane	184.9	0.0021
n-Butane	212.6	0.0017
i-Butane	203.9	0.0070
n-Pentane	234.8	0.0032
i-Pentane	230.2	0.0049
n-Hexane	253.8	0.0046
n-Octane	284.3	0.0073
n-Decane	308.8	0.0091

k_{12} values of CO_2–alkane pairs were determined at the triple point of CO_2 for C_2–C_4 alkanes and at a reduced temperature 0.5 for heavier ones (see Table 2). They are almost constant, what justifies a universal value 0.133, as for ethane and propane.

For CO_2–aromatic pairs the aromatic fractions of hydrocarbons vary, so k_{12} values should be determined separately for each pair. But values given in Table 3 look rather constant, with the exception of benzene, so a constant value 0.10 from toluene on could be justified, at least for CO_2–alkylbenzene pairs.

For methane–alkane pairs the normal boiling point of methane, 111.6 K is always too low, so k_{12} values are calculated at a reduced temperature equal to 0.5 for the heavier component (Table 4). Note that they are all close to zero, what justifies a general assumption of zero values.

6. Conclusions

The classical quadratic mixing rules of the SRK EoS were rewritten as Huron–Vidal mixing rules. Infinite-pressure excess properties can be predicted by group contributions, whose number was sharply reduced by introducing the concept of main groups, like in the UNIFAC method. Hydrocarbon systems, with the exception of methane, can all be described by two main groups only, whose interactions are expressed by one temperature-dependent

parameter. Methane, CO_2, N_2, H_2S are treated as separate groups and their interactions with hydrocarbons are expressed by two parameters for each pair with alkyl and aromatic groups. The final expressions of the interaction parameters are given by Eqs. (12)–(26):

$$\tau\left(\frac{\text{aromatic}}{\text{alkane}}\right) = \left(\frac{72}{T}\right)^2 \quad (12)$$

$$\tau\left(\frac{CH_4}{\text{alkanes}}\right) = \left(\frac{29}{T}\right)^2 \quad (13)$$

$$\tau\left(\frac{CH_4}{\text{aromatic}}\right) = \left(\frac{100}{T}\right)^2 \quad (14)$$

$$\tau\left(\frac{CH_4}{CO_2}\right) = \left(\frac{110}{T}\right)^{1.6} \quad (15)$$

$$\tau\left(\frac{CO_2}{\text{alkanes}}\right) = \left(\frac{118}{T}\right)^{1.6} \quad (16)$$

$$\tau\left(\frac{CO_2}{\text{aromatic}}\right) = \left(\frac{116}{T}\right)^2 \quad (17)$$

$$\tau\left(\frac{N_2}{CO_2}\right) = \left(\frac{85}{T}\right)^{1.2} \quad (18)$$

$$\tau\left(\frac{N_2}{CH_4}\right) = \left(\frac{18.0}{T}\right) \quad (19)$$

$$\tau\left(\frac{N_2}{\text{alkane}}\right) = \left(\frac{57}{T}\right)^{1.4} \quad (20)$$

$$\tau\left(\frac{N_2}{\text{aromatic}}\right) = \left(\frac{163}{T}\right)^{1.6} \quad (21)$$

$$\tau\left(\frac{N_2}{H_2S}\right) = \left(\frac{198}{T}\right)^{1.3} \quad (22)$$

$$\tau\left(\frac{CO_2}{S}\right) = \left(\frac{120}{T}\right)^{1.6} \quad (23)$$

$$\tau\left(\frac{CH_4}{H_2S}\right) = \left(\frac{123}{T}\right)^{1.3} \quad (24)$$

$$\tau\left(\frac{H_2S}{\text{alkane}}\right) = \left(\frac{114}{T}\right)^{1.4} \quad (25)$$

$$\tau\left(\frac{H_2S}{\text{aromatic}}\right) = \left(\frac{10}{T}\right) \quad (26)$$

It must be noted that the classical quadratic mixing rules comply with the theoretical requirement of a quadratic dependence on composition of the second virial coefficients. Huron–Vidal mixing rules do not satisfy that condition in general, but they do in this application where the infinite-pressure excess properties are expressed by the Scatchard–Hildebrand equations. In fact the new mixing rules are completely identical to the classical ones, although they are written in a different form for prediction purposes.

The proposed method can predict the phase behaviour and the thermodynamic properties of systems containing hydrocarbons, nitrogen, carbon dioxide, hydrogen sulfide.

Although it was not the scope of this work, it must be recalled that an improvement of calculated densities an enthalpies can be obtained by introducing the well-known Peneloux volume shift, without any modification of the interaction parameters.

When compared to experimental VLE data, the proposed method gave results with accuracy comparable to those by the well-known PSRK method.

List of symbols

T	absolute temperature, K
P	absolute pressure, bar
V	molar volume, m^3/kg mol
R	universal gas constant, 0.083144 m^3 bar/K
a,b	equation of state parameters
k_{12}	correction factor to the geometric mean of two a parameters
x_i	mole fraction of ith component of a mixture
τ	group interaction parameter, nondimensional
m	(suffix) indicates a quantity referred to a mixture
φ_i	fugacity coefficient of ith component

Appendix A. An approximation of the maximum-likelihood principle

When correlating a set of experimental VLE data to find out the best set of parameters, the usual procedure is to look for the parameter set which minimizes the RMS ΔP of bubble-point calculations. That is correct for a single data set at one temperature, but it is not for multiple data sets at different temperatures, whose isotherms have different slopes. The above procedure will give equal weights to all ΔP's, so forcing the steepest isotherms, the ones at lower temperatures, to pass closer to the experimental points, and farther at higher temperatures. Such an unbalance is graphically evident and requires a correction, because it affects the final parameter values.

In correlations made here, the graphical distances of single experimental points from the calculated bubble point curves were assumed to express the inaccuracies of single points. The best parameter set was considered to be the one that minimizes the RMS distance.

Let us consider the $\ln P$–x diagram of a binary system (see Fig. A1).

Starting from the experimental point C, two types of equilibrium calculation can be done: a bubble pressure calculation at the same liquid composition, giving a point $A(x_{exp}, P_{bp})$ below the experimental one; and a flash calculation at the experimental pressure, giving a point $B(x_{flash}, P_{exp})$ aside the experimental one. The first point has an error $\overline{AC} = \Delta \ln P = \ln(P_{pb}/P_{exp})$ (relative-instead of absolute errors are considered, as usual), the second point an error $\overline{CB} = \Delta x = (x_{exp} - x_{flash})$.

If the errors are small, the segment $\overline{AB}$ of the calculated isotherm can be considered rectilinear. Its length is $\overline{AB} = \sqrt{\left(\overline{AC}^2 + \overline{BC}^2\right)}$ and the length of the height $\overline{CH}$ to the hypotenuse, that is the measure of the error we are looking for, is:

$$\varepsilon = \overline{CH} = \overline{AC} \cdot \frac{\overline{BC}}{\overline{AB}} = \frac{\overline{AC}}{\sqrt{1 + (\overline{AC}/\overline{BC})^2}} = \frac{\Delta \ln P}{\sqrt{(1 + (\Delta \ln P/\Delta x)^2}} \quad (A\text{-}1)$$

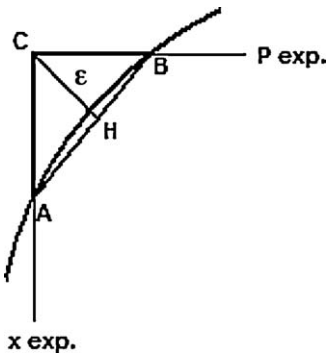

Fig. A1.

That is, the error $\Delta \ln P$ on the bubble point pressure must be scaled by a factor which keeps into account the slope of the $\ln P$–x curve.

The term ε expresses in a more consistent way the inaccuracies related to different data sets.

Further simplifications were introduced here:

a) the term $\Delta \ln P$ was replaced by $\Delta P/P_{exp}$, which for small deviations is almost identical
b) assuming that K-values are inversely proportional to the pressure (correct at lower pressures), it is easy to show that the relative error in the bubble-point pressure is given by:

$$\frac{\Delta P}{P_{exp}} \approx \sum K_i x_i - 1 \tag{A-2}$$

(where K values are calculated at the experimental T, P and phase compositions)

c) assuming that K values are independent on composition (acceptable in absence of strong non-idealities), the liquid–phase concentration in a binary system is:

$$x_{1,calc} = \frac{(1 - K_2)}{(K_1 - K_2)} \tag{A-3}$$

(with K values calculated at the experimental T, P and phase compositions) and the error Δx is:

$$\Delta x = x_{1,calc} - x_{1,exp} \approx \left(\frac{\left(\sum K_i x_i - 1\right)}{(K_1 - K_2)} \right) \tag{A-4}$$

The result of Eqs. (A-2) and (A-4), with some approximation, is thus:

$$\frac{\Delta \ln P}{\Delta x} \approx K_1 - K_2 \tag{A-5}$$

and finally, combining Eqs. (A-1) and (A-5):

$$\varepsilon = \left(\frac{\left(\sum K_i x_i - 1\right)}{\sqrt{1 + (K_1 - K_2)^2}} \right) \tag{A-6}$$

regardless of whether the experimental data set is isothermal or isobaric.

Eq. (A-6) does not require a rigorous calculation of the bubble pressure or temperature. It is enough to calculate K values at the experimental T, P and phase compositions. If the vapour composition is unknown, a frequent case, it is sufficient to calculate it by a single iteration of a simulated bubble-point calculation:

$$y_1 = \frac{K_1 x_1}{\sum K_i x_i} \tag{A-7}$$

with K values calculated at experimental T, P, x and with $y = 1$ for the more volatile component. (iterations can be repeated using final y values, but it is normally useless)

Once a set of ε values is obtained at all experimental point, their sum of the squares (or root mean square, RMS, value, which above was called the weighted RMS ΔP) shall be minimized to determine the best parameter set.

References

[1] G. Soave, Chem. Eng. Sci. 27 (1972) 1197–1203.
[2] A. Maczynski, J. Niezdiela, Polish Acad. of Sciences. Floppy Book on Vapour–Liquid Equilibrium Data of Organic Compounds and Water, TRC, Texas A&M University System, College Station, USA, 1992.
[3] T. Holderbaum, J. Gmehling, Fluid Phase Equilib. 70 (1991) 251–265.
[4] A. Jabłoniec, S. Horstmann, J. Gmehling, Ind. Eng. Chem. Res. 46 (2007) 4654–4659.
[5] M.J. Huron, J. Vidal, Fluid Phase Equilib. 3 (1979) 255–271.
[6] J.H. Hildebrand, R.L. Scott, Regular Solutions, Prentice-Hall, Englewood Cliffs, New Jersey, 1962.
[7] A. Fredenslund, J. Gmehling, P. Rasmussen, Vapor–Liquid Equilibria Using UNIFAC: A Group Contribution Method, Elsevier, Amsterdam, 1977.
[8] G.M. Wilson, C.H. Deal, Ind. Eng. Chem. Fundam. 1 (1962) 20–23.
[9] D.S. Abrams, J.M. Prausnitz, AIChE J. 21 (1975) 116–128.
[10] G. Soave, Fluid Phase Equilib. 31 (1986) 203–207.
[11] Aspen Physical Property System, Physical Property Methods, Physical Property Models, AspenONE Documentation, Aspen Technology Inc., Burlington, MA, 2009.
[12] J.W. Glanville, B.H. Sage, W.N. Lacey, Ind. Eng. Chem. 42 (1950) 508–513.
[13] H.H. Reamer, B.H. Sage, W.N. Lacey, Ind. Eng. Chem. 42 (1950) 534–539.
[14] D. Legret, D. Richon, H. Renon, J. Chem. Eng. Data 27 (1982) 165–169.
[15] H.M. Lin, H.M. Sebastian, J.J. Simnick, K.C. Chao, J. Chem. Eng. Data 24 (1979) 146–149.
[16] G.I. Kaminishi, C. Yokoyama, S. Takahashi, Fluid Phase Equilib. 34 (1987) 83–99.
[17] H. Inomata, K. Arai, S. Saito, Fluid Phase Equilib. 36 (1987) 107–119.
[18] R. Stryjek, P.S. Chappelear, R. Kobayashi, J. Chem. Eng. Data 19 (1974) 340–343.
[19] L. Grausø, A. Fredenslund, J. Mollerup, Fluid Phase Equilib. 1 (1977) 13–26.
[20] P. Miller, B.F. Dodge, Ind. Eng. Chem. 32 (1940) 434–438.
[21] H. Kalra, D.B. Robinson, T.R. Krishnan, J. Chem. Eng. Data 22 (1977) 85–88.
[22] S. Laugier, D. Richon, J. Chem. Eng. Data 40 (1995) 153–159.
[23] H.J. Ng, H. Kalra, D.B. Robinson, H. Kubota, J. Chem. Eng. Data 25 (1980) 51–55.